Ann. For. Res. 65(1): 12221-12236, 2022
ISSN: 18448135, 20652445

ANNALS OF FOREST RESEARCH
https://www.e-afr.org/

THERMAL CHARACTERISTICS OF INCLINED WATER JET INTELLIGENT COOLING SYSTEM ON HOT TARGET

Raj Bahadur Singh
Research Scholar, Glocal University, UP, India
brsingh2020@yahoo.in

Prof. Dr. Beg Raj Singh
Supervisor / Guide, Glocal University India.
begrajsingh14@gmail.com

Prof. Sunil B. Ingole
Co-Guide, Director and Prof. in Mechanical Engg, Indira college of Engineering and Management, Pune, India 410506, sbingole1@rediffmail.com

Abstract

High-pressure water jet technology is currently highly significant in the automotive cleaning sector. Due to an inappropriate arrangement of nozzles on their spray rods, certain automated washers are unable to fulfil the washing requirements throughout the washing process. In this study, the internal and exterior flow field models of the nozzle are created using the computational fluid dynamics (CFD) theory. The flow field is simulated and examined using Fluent, and the external nozzle settings on the side spray bar of the automatic car washer are optimised. According to the modelling findings, when the nozzle and the normal line of the automotive surface are angled at a specific angle, the target surface is also subjected to tangential pushing force in addition to normal hitting force, which makes stains easier to remove. The nozzle should be angled away from the typical line of the automotive surface by 30° for the greatest washing results. The dynamic pressure on the surface of the car will rise as the nozzle inlet pressure rises, but after reaching a certain pressure, the rise in dynamic pressure will fall. The region covered by the water jet is mostly unaffected by the intake pressure. In addition to completely covering and cleaning the automobile surface, the reasonable matching results of jet angle, nozzle spacing, and nozzle distance from the automobile surface (target distance) obtained by numerical simulation can also ensure less jet interference and no water waste from nearby nozzles. The aforementioned study findings can serve as a fundamental theoretical foundation for the best automatic car washing design.

Key: Thermal, Characteristics, Inclined, Water, Jet, Intelligent, Cooling, System, Hot, Target.

Introduction

The number of cars is rising quickly along with society's progress, and so is the amount of study being done on vehicle maintenance [1, 2]. The daily washing quantity and frequency are the most common among them [3]. Historically, hand washing was unable to keep up with the great volume

© ICAS November 2022

and frequency of automotive cleaning. Currently, there are two types of automatic car washing: contact type and noncontact type. Despite the fact that stains on a car may be easily removed with contact type, hard particles (such as sand,

The washing head will become entangled with small stones and thin steel wires (which are frequently present in stains on the car, causing harm to the car). The noncontact type does not damage the car through friction by using high-pressure water blasted by high-pressure fan-type nozzles for washing. The primary automotive washer technique is high-pressure water jet cleaning [4, 5]. It has a wide variety of applications, a high decontamination capability, produces no environmental pollution, and is simple to automate [6–10]. It serves as the foundation for the industry's automated control [11–14]. High-pressure water flow is expelled from the nozzle of the high-pressure jet washer by means of a high-pressure pump [8, 15, 1].

Water Jet Distribution Structure of Automobile Washing Nozzle

Figure depicts the spray rod and nozzle of an automatic car washer physically. Figure depicts the nozzle water jet structure [3][1]. Due to the enormous speed differential between the water jet an d the surrounding air after it is released from the nozzle's slit and the exchange of mass and energ y with the air, the ejected water jet continually diffuses to the surroundings. The jet's border then becomes wider, its velocity drops, and the region where it maintains its original velocity is likewi se continually decreasing. The outer edge of the jet is the barrier with zero velocity.

Figure 1 : The physical diagram of the side spray bar of an automatic automobile washer.

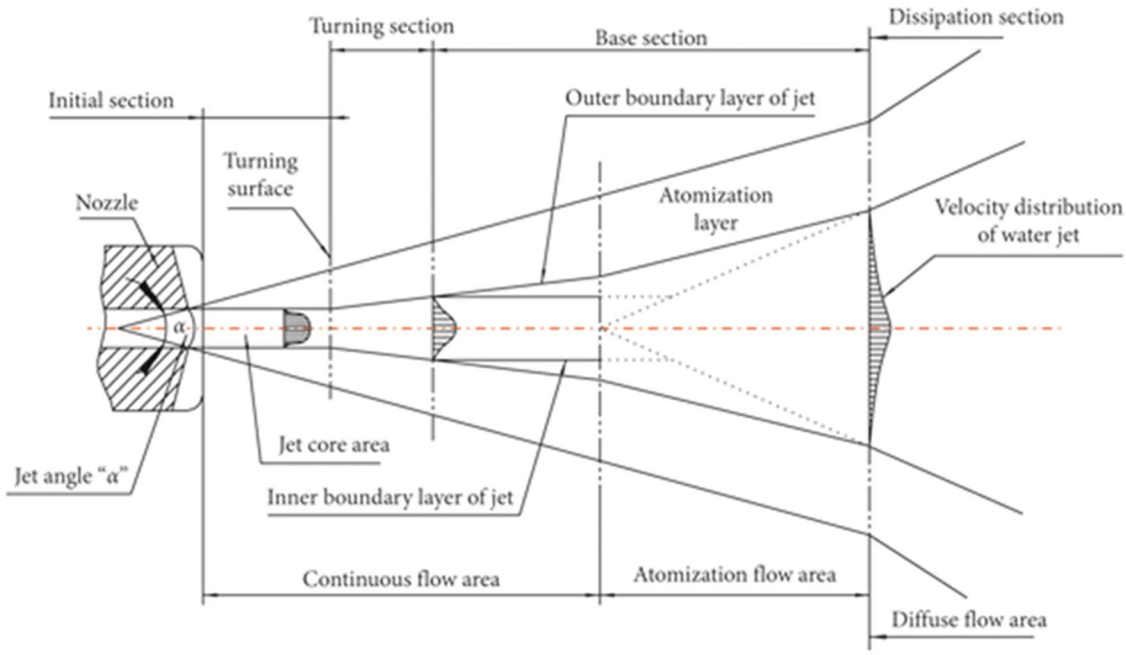

Figure 2 : The jet distribution structure diagram of the nozzle.

The starting portion, the fundamental section, and the dissipation section from the nozzle output are basically the three jet sections that make up the water jet. The first part of the water jet is the segment that extends from the nozzle's outflow to the point at which the velocity core completely vanishes. In the vicinity of the jet core, the axial dynamic pressure, velocity, and density essentially stay unaltered. As a result, cutting material is often done using the water jet's beginning segment. The area where the velocity core zone is eliminated from the water jet's early segment is known as the mixing zone.

Mathematical Model

For high-pressure water jet washing, assuming that water is an incompressible steady-state flow, the continuity equation iswhere , , and are the three velocity components of x, y, and z, respectively, m/s. The momentum equation iswhere f_x, f_y, and f_z are the components of unit mass force on 3 coordinate axes, respectively; ρ is the density of water, kg/m^3; μ is the dynamic viscosity of water, kg/m·s. Water jet automobile washing belongs to the gas-liquid two-phase flow movement. First of all, it is necessary to judge whether it is a laminar flow or turbulent flow. In multiphase flow, each relevant parameter can be expressed by the following equation:where R_e is the Reynolds number; is the velocity of water at the nozzle inlet, m/s, generally about 100 m/s; D is the diameter of nozzle inlet, about 3 mm; $\mu = 0.001$ kg/m·s.

© ICAS November 2022

3D Model

The high-pressure water jet discussed in this paper belongs to obvious gas-liquid two-phase flow with obvious interface stratification, and the jet also belongs to free-surface flow. Based on the above mathematical model, VOF model and standard turbulent k–ε model are selected for analysis in simulation.

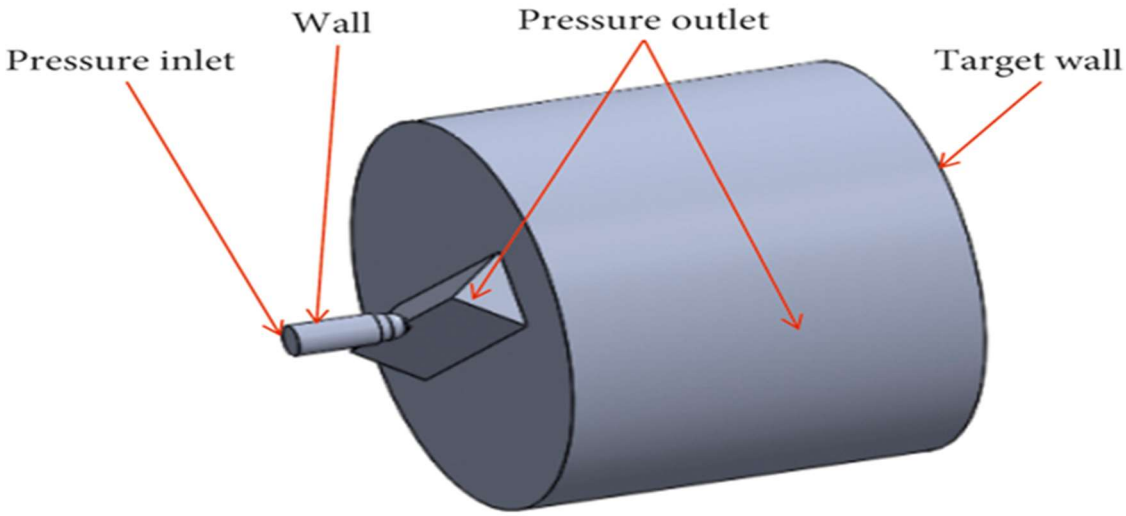

Figure 3: 3D model of nozzle and external flow field.

Mesh Generation and Fluent Boundary Condition Setting

Tetrahedral and hexahedral mesh are joined, the mesh is encrypted at nozzles and triangular pris ms, and an expansion layer is built up at the outflow field during the mesh division process. Final ly, the mesh quality measurement indicates that the scenes of the mesh are around 0.2, indicating that it falls within the category of "very good." The numerical range of orthogonal mass is 0–1; th e closer to 1, the better. The orthogonal mass is around 0.9. Above evidence demonstrates that th e lattice quality satisfies the criteria [3][2].

© ICAS November 2022

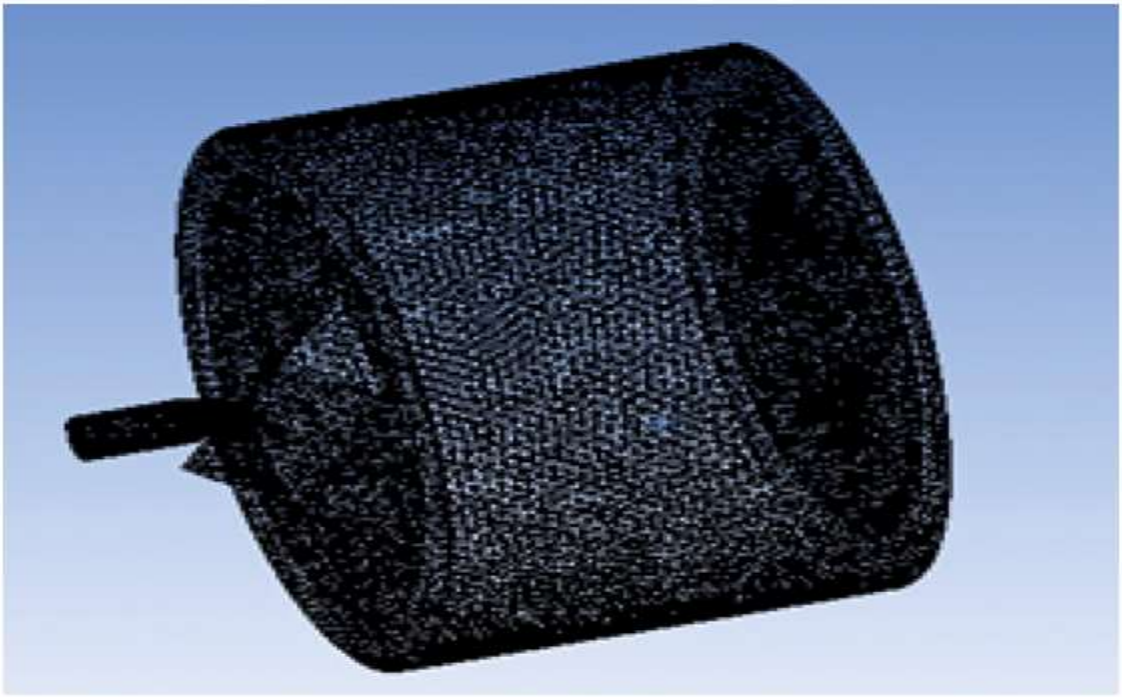

Figure 4 : Mesh model of nozzle and external flow field.
Figure depicts the border condition setup. Since air first occupies the whole outflow field, air is chosen as the primary phase and water fluid as the second phase to address the issue as closely as possible. In other words, the nozzle is initially filled with water, the outlet pressure is set to 1 atmosphere (i.e., the relative static pressure is zero), and the external flow field is initially filled with air. The inlet boundary pressure of the nozzle is chosen to be 6-12 MPa, and the volume fraction of inlet water is set to be 1. The surface of the wall uses a standard nonslip wall surface, the function of the standard wall surface replicates the near-wall effect, and the SIMPLE

Verify the Correctness of the Model

For continuous jet, the Bernoulli equation is adopted between the inner and outer two points of nozzle outlet cross section, ignoring the height difference between the two points, and the following relation [3][4] can be obtained: where p_1 and p_2 are the static pressure inside and outside the nozzle; and are the average flow velocity inside and outside the nozzle.

Applying the continuous equation to two points, the following relation can be obtained:
For the convenience of theoretical analysis, the nozzle flow path can be a circular tube structure; that is, $A = \pi d^2/4$; assuming $\rho_1 = \rho_2$, the following relationship can be deduced by combining (5) and (6):

© ICAS November 2022

For the water jet used for washing, because $p_1 >> p_2$, $(d_2/d_1)^4 << 1$, and $\rho = 998$ kg/m^3, the relevant values are substituted into (7), and the simplified expression of jet velocity is obtained: where p is the static pressure at the nozzle inlet; is the nozzle outlet velocity.

From equation (8), when the static pressure at the inlet is 8 MPa, the velocity at the outlet of the nozzle is 126.60 m/s.

In order to verify the correctness of the simulation model, it is necessary to compare the value calculated by the above formula with the simulation result. Therefore, both solutions are set as the static inlet pressure 8 MPa. The simulation results are as shown in Figure . The velocity at the nozzle outlet is 127.40 m/s according to the velocity nephogram. The error $\Delta = (127.4–126.6)/126.6 = 0.632\%$. The simulation results are very close to the theoretical calculation results, which show that the model is reliable.

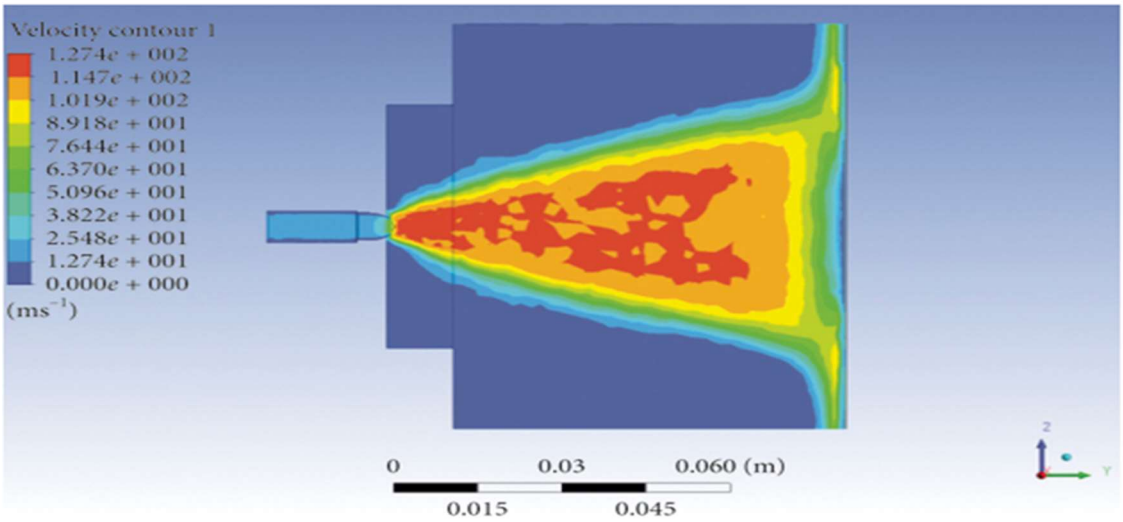

Figure 5: Water jet velocity reprogram with inlet pressure of 8 MPa.

Simulation Analysis and Comparison of Different Target Distances

As can be seen from Figure, the water jet velocity and dynamic pressure in the basic section gradually decrease with the axial target distance (the distance from the nozzle outlet to the automobile surface). Obviously, the choice of target distance has a great influence on the washing effect. The dynamic pressure on the target surface is an important characteristic of water jet, which represents the striking force of water jet on the target surface.

The inlet pressure is selected to be 8 MPa, and the external flow field is simulated and analyzed under the conditions that the target distances are 60 mm, 70 mm, 80 mm, and 100 mm, respectively. The dynamic pressure cloud images of the target surface under different target

distances are obtained as shown in Figure, and the radial dynamic pressure curves of the target surface under different target distances.

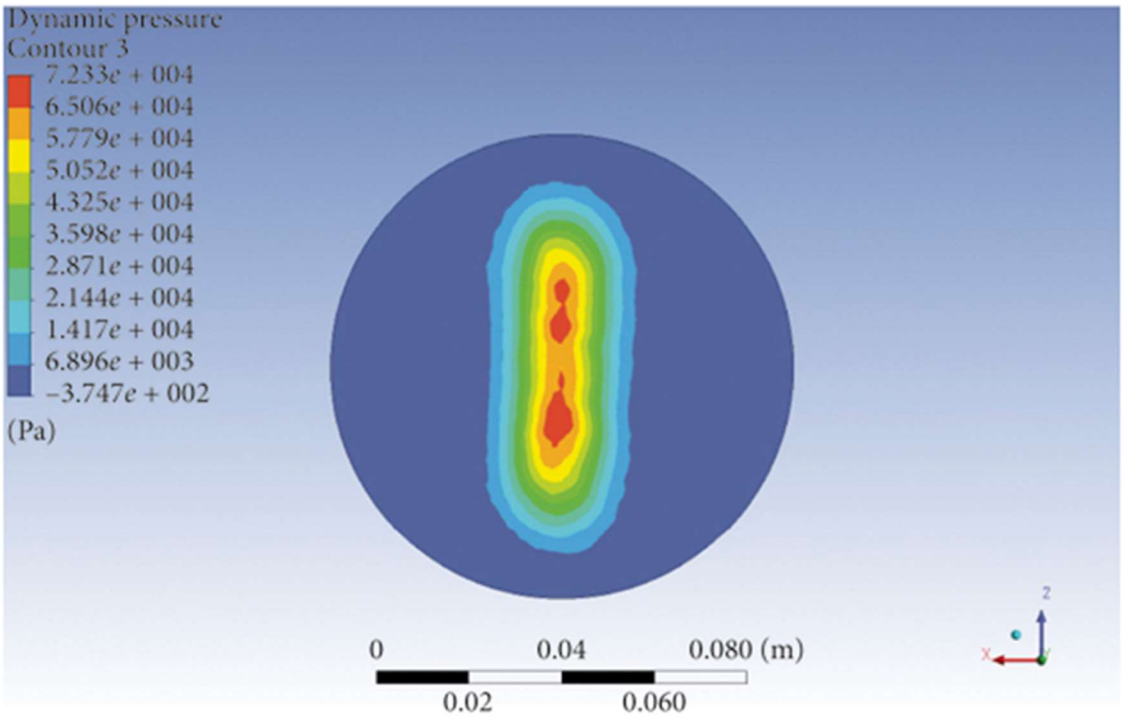

Figure 6 : Dynamic pressure reprogram of target surface at different target distances.

Although the water jet's capacity to wash reduces as the target distance grows, the water jet's coverage area expands along with the amount of the car that can be cleaned. Figures show that when the target distance is 60 mm, the water jet that reaches the target surface has a reverse impact force that partially cancels the forward water jet because the nozzle is too close to the surface of the car, causing the dynamic pressure on the target surface to be uneven. The dynamic pressure on the target surface starts to decline as the target distance increases, however the no uniformity of the dynamic pressure value is noticeably lessened.

Comparison of Simulation Analysis of Different Inlet Pressures

The target distance is 70 mm, and the external flow field is simulated under the conditions of inlet pressures of 6 MPa, 8 MPa, 10 MPa, and 12 MPa, respectively. The dynamic pressure nephogram of the target surface under different inlet pressures is obtained as shown in Figure, and the axial velocity distribution under different inlet pressures is shown in Figure.

© ICAS November 2022

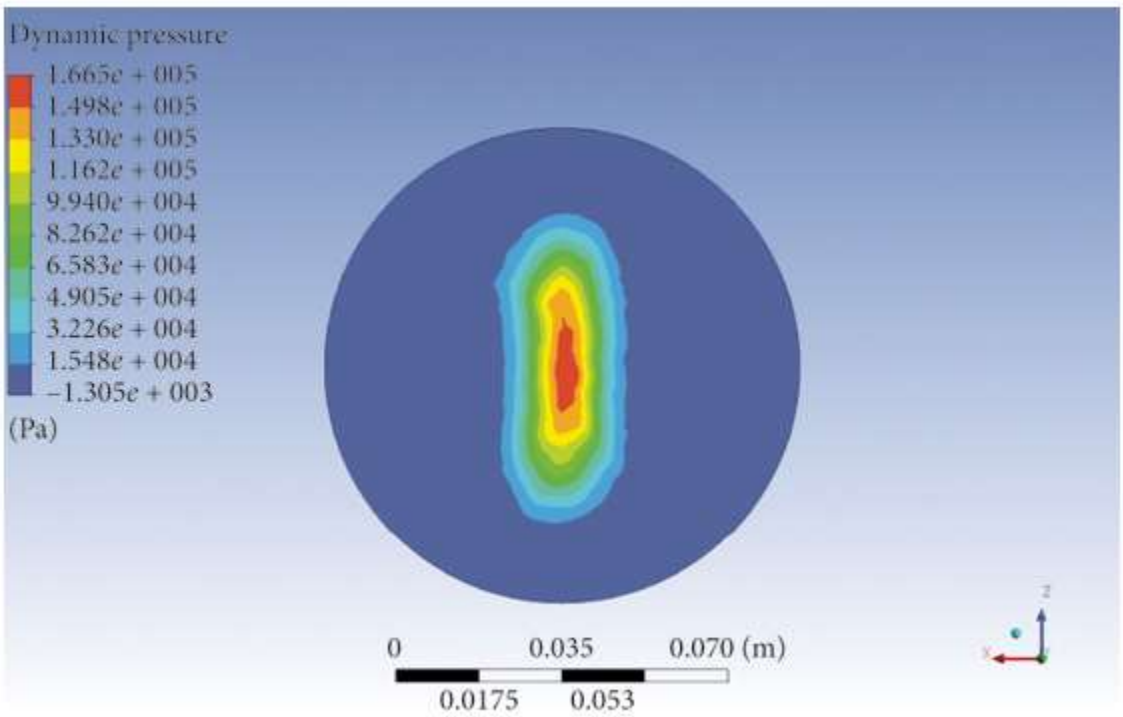

Figure 7: Target dynamic pressure reprogram under different inlet pressure.

As can be seen from Figure, when the inlet pressure changes from 6 MPa to 8 MPa, the target surface dynamic pressure increase rate is 33.18%, when the inlet pressure changes from 8 MPa to 10 MPa, the target surface dynamic pressure increase rate is 24.89%, and when the inlet pressure changes from 10 MPa to 12 MPa, the target surface dynamic pressure increase rate is 19.78%. It can be concluded that the increase rate of the dynamic pressure on the target surface decreases with the increase of the inlet pressure; under the condition of a certain target distance, the area covered by water jets with different inlet pressures is basically the same. As seen in

Simulation Analysis and Comparison of Different Included Angles

At present, the spray rod nozzle of the car wash is perpendicular to the surface of the automobile, so that the surface of the automobile is mainly subject to normal strike force and little tangential strike force during the washing process, and some stubborn stains are not easy to be cleaned off. In the process of water jet washing, it should be considered that inclining the jet direction of the nozzle to the target surface (automobile surface) at a certain angle will greatly enhance its washing effect. In order to realize the simulation of outflow field under different included angles, the normal included angles between nozzle and target surface are 0°, 15°, 30°, and 45° through different angles of target surface inclination. The schematic diagram of the model is shown in Figure, and the 3D model is shown in Figure.

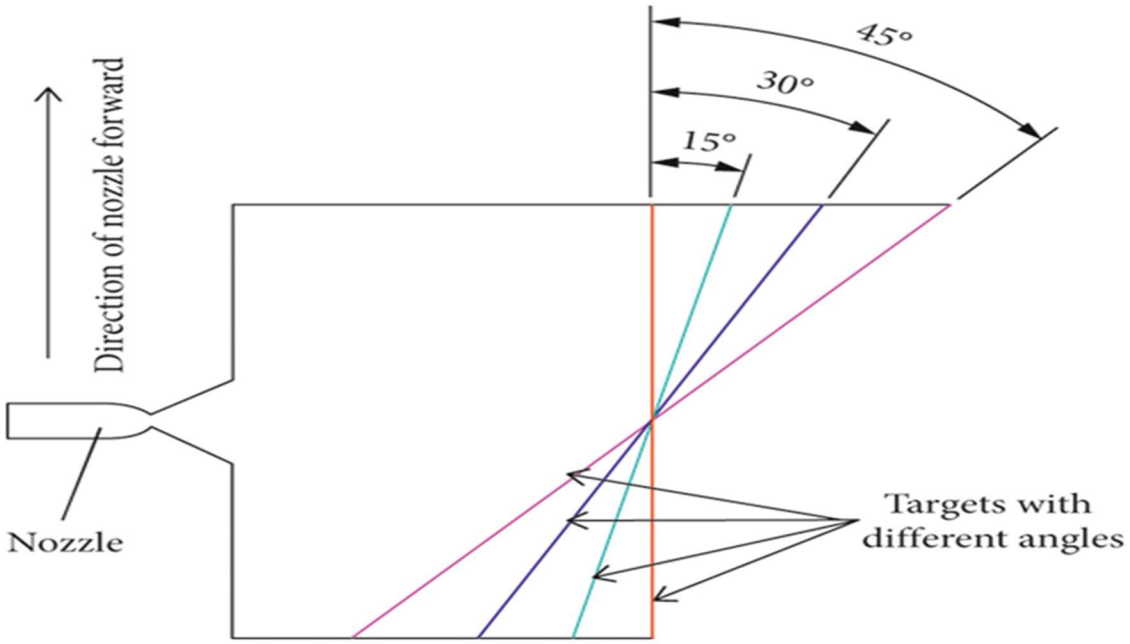

Figure 8: Model schematic diagram different from normal angle of target surface

.

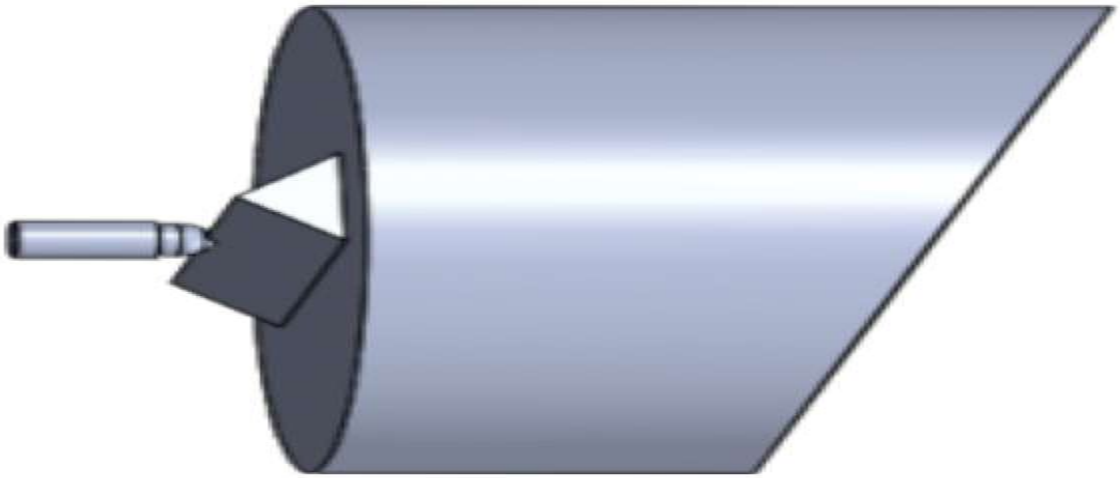

Figure 9: 3D model with inclined angle.

By observing Figure it can be seen that when the inclination angle is 0°, the speed of the water jet reaching the target surface in the tangential advancing direction is very small. After inclining by a certain angle, the speed of the water jet reaching the target surface in the tangential advancing direction of the nozzle gradually increases and reaches the maximum when the inclination angle is 30°. Therefore, considering the velocity distribution and the dynamic pressure of the target surface comprehensively, 30° is taken as the optimal included angle.

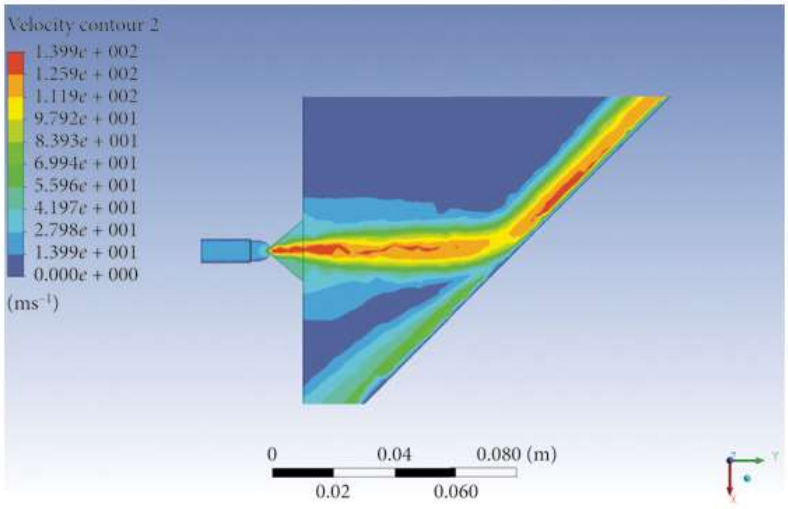

Fig: 10: Velocity reprogram at different angles. (a) 0°. (b) 15°. (c) 30°. (d) 45°.

Comparison of Simulation Analysis with Different Spacing

When arranging nozzles, the influence of nozzle spacing on the external flow field should be considered. If the nozzle spacing is too small, the edge water jet of the fan-type external flow field will interfere, thus affecting the washing effect. If the nozzle spacing is too large, the fan-type outflow field cannot cover all washing surfaces and cannot meet the washing requirements. In this paper, the nozzle spacing is simulated by establishing a 3D model.

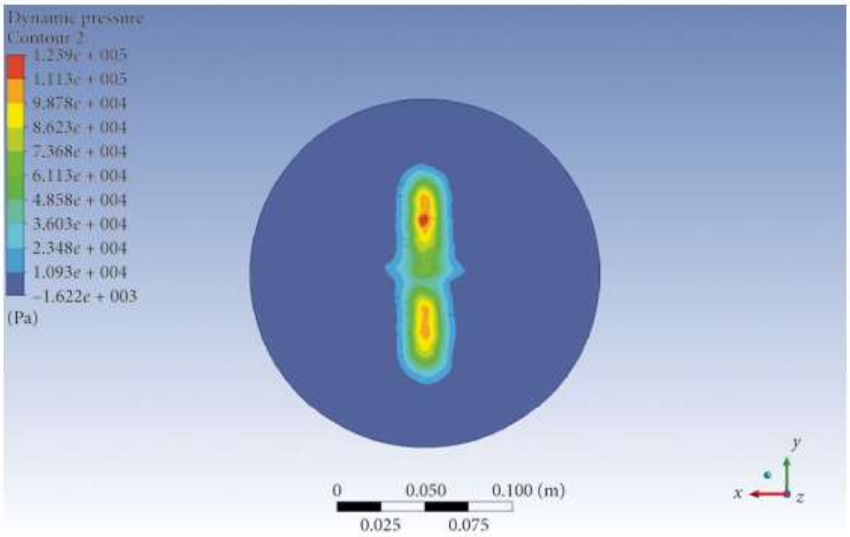

(d) Figure 12: Dynamic pressure echograms of target surfaces with different spacing. (a) 100 mm. (b) 80 mm. (c) 70 mm. (d) 60 mm.

© ICAS November 2022

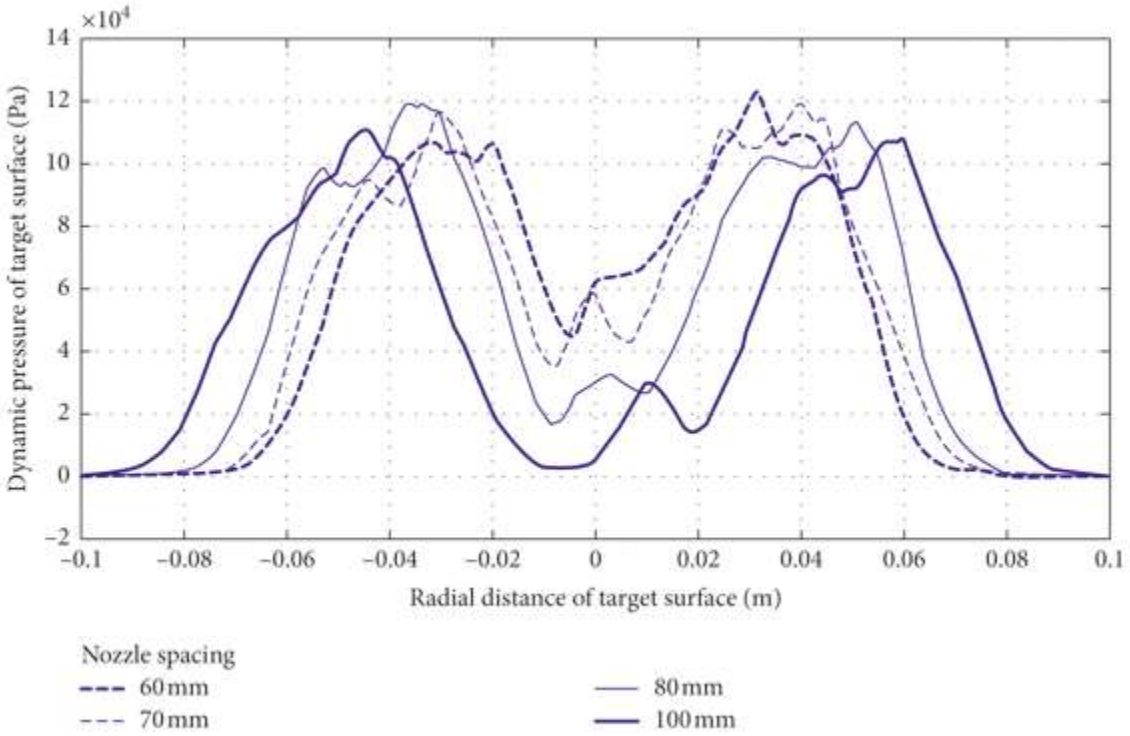

Figure 13: Radial dynamic pressure of target surface at different spacing.

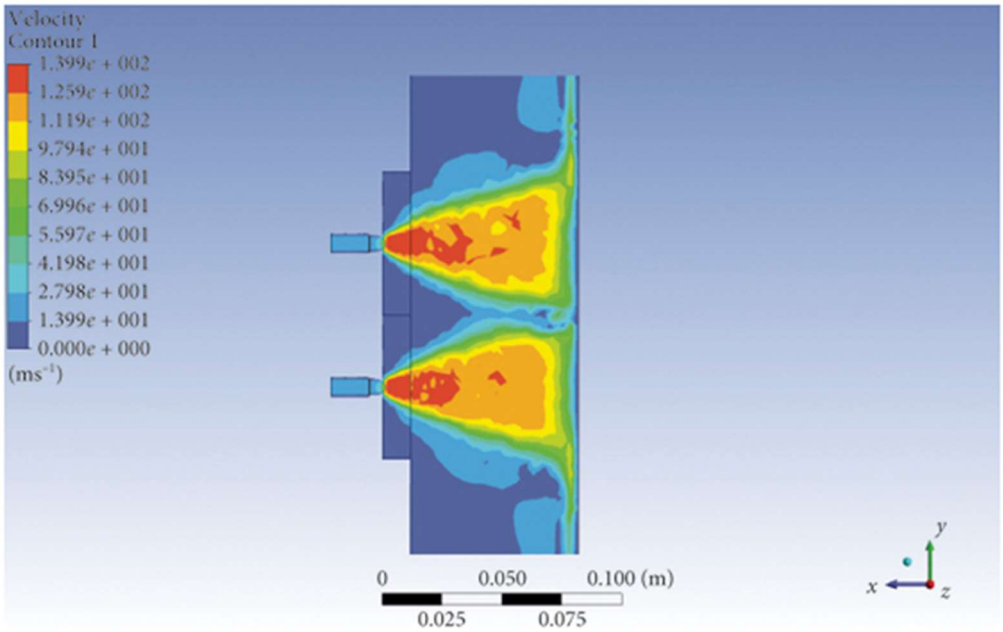

Figure 14 : Velocity nephogram with different spacing. (a) 100 mm. (b) 80 mm. (c) 70 mm. (d) 60 mm.

Relationship between Target Distance and Shooting Width under Different Jet Angles

When the jet angle α is 15°, 30°, 45°, and 60° and the target distance is adjusted to 50 mm, 100 mm, 150 mm, 200 mm, 250 mm, 300 mm, 350 mm, 400 mm, 450 mm, and 500 mm, respectively, the shooting width is investigated to find out the matching relationship between the target distance and the shooting width. The solution result is shown in Figure.

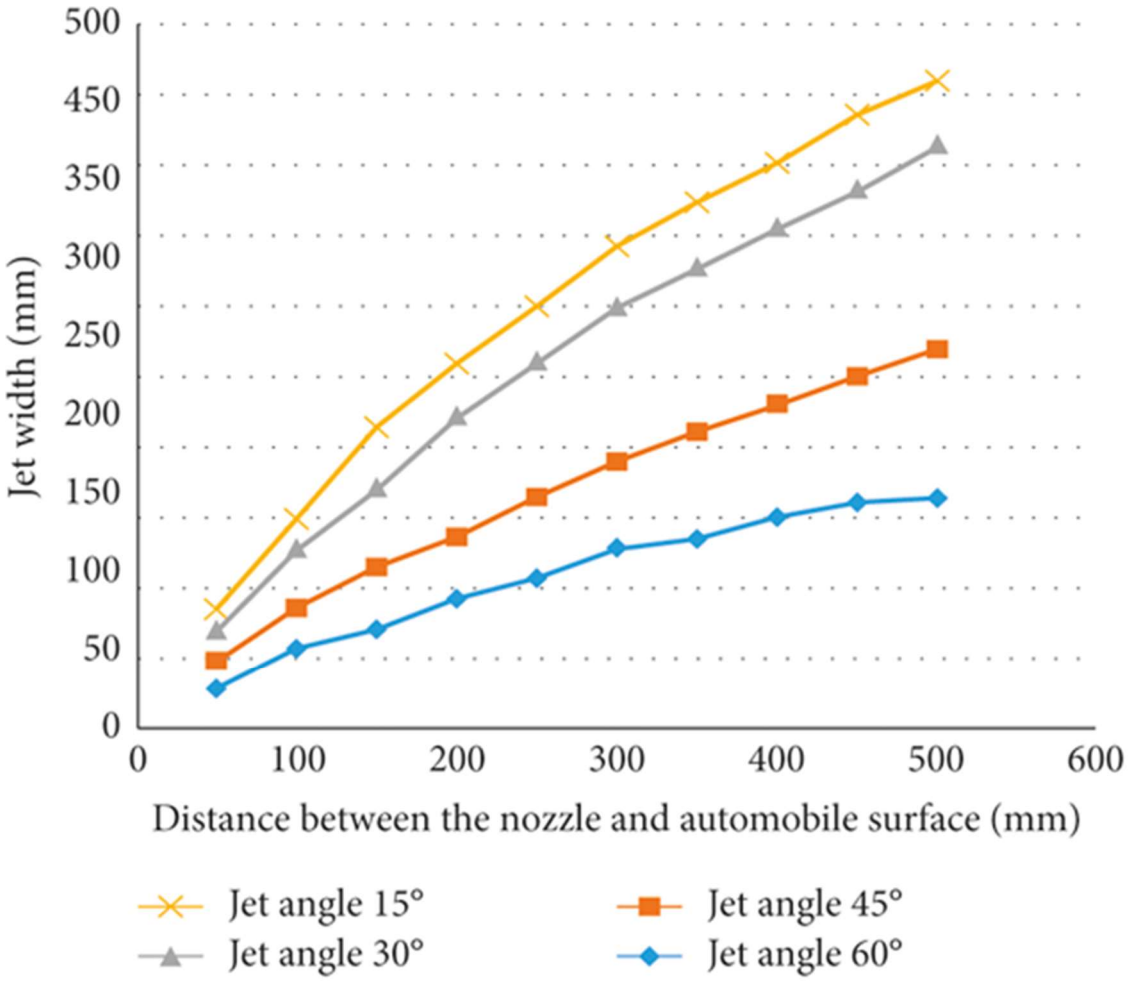

Figure 15 : Relationship curve between jet target distance and jet width under different jet angles

.

However, Figure can be used as the theoretical basis for matching the jet angle, nozzle spacing, and the distance between the nozzle and the automobile surface (target distance). In actual automobile washing, the nozzle spacing on the spray rod is generally premade (it will not change during automobile washing). If the nozzle spacing is too small, the jet coverage area can be effectively increased, but the number of nozzles on the spray rod of the same length will inevitably increase and the water consumption will also rise sharply. As can be seen from Figure, when the

© ICAS November 2022

nozzle spacing is too large, part of the automobile surface cannot be covered by water jet. Therefore, when washing the car, the distance (target distance) between the nozzle on the spray rod and the surface of the automobile can be adjusted to ensure that the jet width value is always greater than the nozzle spacing, thus achieving the purpose of washing without dead corners

Test Verification

Since the impact force of water jet on the automobile cannot be accurately detected, the cleanliness of the automobile is used to check whether the impact force is appropriate. Taking an automatic automobile washing workshop as the test object, the original automatic automobile washer has 15 nozzles with an incidence angle of 45°, a distance between the nozzle and the automobile on the automobile washing spray rod of about 300 mm, a normal angle between the nozzle jet direction and the target surface (automobile surface) of 0°, and a distance between adjacent nozzles of 150 mm.

Figure 16 : Layout of on-site automatic automobile washer.

Under the same condition of washing the automobile, the following conclusions can be drawn through the comparison before and after the renovation: (1) The water consumption after the renovation is saved by about 46% compared with that before the renovation, thus solving the problem of large water consumption on-site. (2) The distance between nozzles before modification

is too small, resulting in serious cross interference of water jets between adjacent nozzles, and the utilization rate of nozzle water jet washing capacity is greatly reduced as shown in Figure.

The modified nozzle water jet not only covers the surface of the automobile but also greatly improves the efficiency of each nozzle water jet. (3) When the normal angle between the nozzle jet and the automobile surface is 0° before the renovation, stains will be scattered and washed away on the automobile surface, and some stains will be washed to the washed automobile parts, causing secondary pollution to them. After reforming the normal included angle between the nozzle jet and the automobile surface to 30°, the nozzle water jet is decomposed into normal striking force and tangential pushing force.

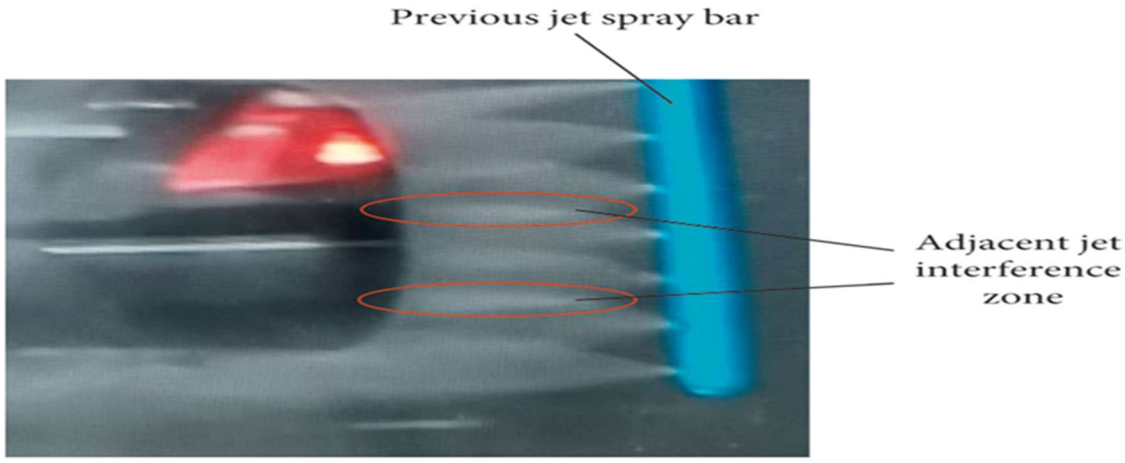

Figure 17 Nozzle jet before modification.

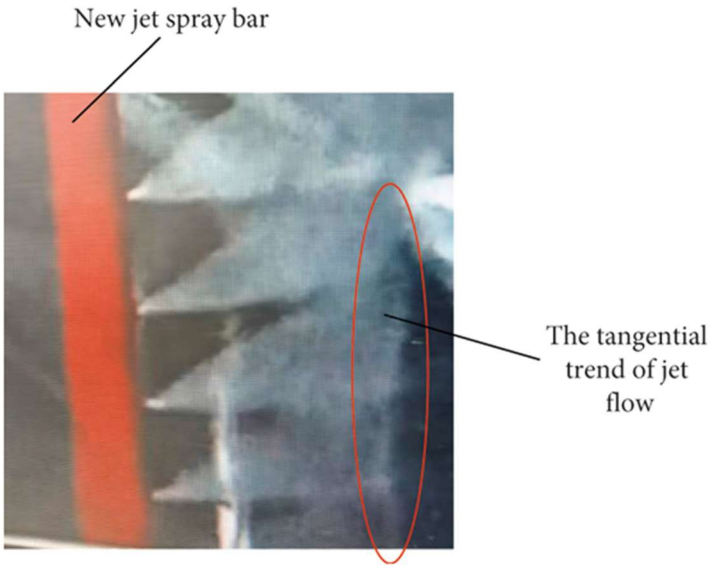

Figure 18 Water accumulation diagram caused by excessive pressure.

Conclusion

The fan-type nozzle is more and more widely used in automobile washing industry. In order to achieve the best washing effect, this paper uses Fluent software to simulate the outflow field of the fan-type nozzle of the automobile washer, analyzes and discusses the influence of the inlet pressure of the nozzle on the spray rod, the target distance, the normal included angle between the nozzle and the body surface, and the nozzle arrangement spacing on the washing effect, and draws the following conclusions:(1)Under the same inlet pressure, the dynamic pressure on the target surface decreases with the increase of the target distance, but too close, the target distance will cause a reverse impact force of the water jet reaching the target surface to partially offset the forward water jet reaching the target surface, making the dynamic pressure on the target surface uneven. The distance between the target surfaces should be determined by comprehensively considering the uniformity of the dynamic pressure on the target surface and keeping the target surface with large dynamic pressure. Although the larger the target distance, the weaker the washing ability of the water jet, the larger the coverage area of the water jet, the larger the area of the automobile that can be cleaned.(2)With the increase of inlet pressure, the dynamic pressure on the target surface and the axial velocity will increase, but the growth rate will gradually decrease when reaching a certain pressure.

References

1. K. Jiang, F. Yan, and H. Zhang, "Data-driven modeling and UFIR-based outlet NO_x estimation for diesel-engine SCR systems," *IEEE Transactions on Industrial Electronics*, vol. 67, no. 6, pp. 5012–5021, 2020.
2. K. Jiang, F. Yan, and H. Zhang, "Hydrothermal aging factor estimation for two-cell diesel-engine SCR systems via a dual time-scale unscented Kalman filter," *IEEE Transactions on Industrial Electronics*, vol. 67, no. 1, pp. 442–450, 2020.
3. M. Kierzkowski and H. Law, "Car wash noise and EPA regulation—a case study," in *Proceedings of the ACOUSTICS 2017 Perth: Sound, Science and Society—2017 Annual Conference of the Australian Acoustical Society, AAS 2017*, Perth, Australia, November 2017.
4. A. Nair and S. Kumanan, "Optimization of size and form characteristics using multi-objective grey analysis in abrasive water jet drilling of Inconel 617," *Journal of the Brazilian Society of Mechanical Sciences and Engineering*, vol. 40, no. 3, pp. 1–15, 2018.
5. S. Thomas, M. Antony, and T. Dimitra, "Hard rock cutting with high pressure jets in various ambient pressure regimes," *International Journal of Rock Mechanics and Mining Sciences*, vol. 108, no. 8, pp. 179–188, 2018.
6. D. Hu, X.-H. Li, C.-L. Tang, and Y. Kang, "Analytical and experimental investigations of the pulsed air-water jet," *Journal of Fluids and Structures*, vol. 54, pp. 88–102, 2015.
7. S. Hannes, K. Hannes, M. Marc, and J. P. Majschak, "Investigations to increase washing efficiency with pulsed liquid jet," *Chemie Ingenieur Technik*, vol. 86, no. 5, pp. 707–713, 2014.
8. L. M. Hlaváč, "Application of water jet description on the de-scaling process," *International Journal of Advanced Manufacturing Technology*, vol. 80, no. 5–8, pp. 721–735, 2015.

© ICAS November 2022

9. F. Enrico, K. Sebastian, and S. Enrico, "Effect of industrial scale stand-off distance on water jet break-up, washing and forces imposed on soil layers," *Food and Bioproducts Processing*, vol. 113, no. S1, pp. 129–141, 2019.
10. E. Helal, F. S. Abdelhaleem, and W. A. Elshenawy, "Numerical assessment of the performance of bed water jets in submerged hydraulic jumps," *Journal of Irrigation and Drainage Engineering*, vol. 146, no. 7, 2020.
11. A. Janardanan, P. C. Ajil, P. Anju, T. V. Eldiya, and D. Davis, "Android application for car wash services," in *Proceedings of 1st International Conference on Emerging Trends and Innovations in Engineering and Technological Research*, Cochin, India, July 2018.
12. D. Phipps, R. Alkhaddar, and M. Stiller, "Water saving in domestic car washing," in *Proceedings of World Environmental and Water Resources Congress 2013: Showcasing the Future*, Cincinnati, OH, USA, May 2013.
13. T. T. Yu, J. Q. Wang, L. T. Wu, and Y. Xu, "Three-stage network for age estimation," *CAAI Transactions on Intelligence Technology*, vol. 4, no. 2, pp. 122–126, 2019.
14. R. Jiang, H. Zhou, H. Wang, and S. S. Ge, "Maximum entropy searching," *CAAI Transactions on Intelligence Technology*, vol. 4, no. 1, pp. 1–8, 2019.
15. C. L. Tang, D. Hu, and F. H. Zhang, "Study on the frequency characteristic of self-excited oscillation pulsed water jet," *Advanced Materials Research*, vol. 317–319, pp. 1456–1461, 2011.
16. E. Fuchs, H. Köhler, and J. P. Majschak, "Measurement of the impact force and pressure of water jets under the influence of jet break-up," *Chemie Ingenieur Technik*, vol. 91, no. 4, pp. 455–466, 2019.
17. J. W. Wen, Z. W. Qi, and S. S. Behbahani, "Research on the structures and hydraulic performances of the typical direct jet nozzles for water jet technology," *Journal of the Brazilian Society of Mechanical Sciences and Engineering*, vol. 41, no. 12, p. 570, 2019.

© ICAS November 2022